16th World Conference on Earthquake, 16WCEE 2017

Santiago Chile, January 9th to 13th 2017

Paper N° 4303 (Abstract ID)

Registration Code: S-U1463235509

SEISMIC PERFORMANCE OF POST-TENSIONED STEEL FRAMES WITH HYSTERETIC DISSIPATERS.

A. López-Barraza[1,*], A. Reyes-Salazar[1], S. E. Ruiz Gómez[2], J. L. Rivera Salas[1], Luis Lugo-Bastidas[3]

(1) *Professor, Facultad de Ingeniería, Universidad autónoma de Sinaloa, Ciudad Universitaria, Culiacán, Sinaloa, México, alopezb@uas.edu.mx, reyes@uas.edu.mx, luz@uas.edu.mx*

(2) *Professor, Instituto de Ingeniería, Universidad Nacional Autónoma de México, Ciudad Universitaria, Coyoacán, México, D.F., SRuizG@iingen.unam.mx*

(3) *Student, Facultad de Ingeniería, Universidad autónoma de Sinaloa, Ciudad Universitaria, Culiacán, Sinaloa, México, luisillo_lugo93@hotmail.com*

Abstract

A comparison of the structural performance of Post-Tensioned Steel Frames (PTSF) and Steel Frames with Welded Connections (rigid) (SFWC) under seismic action is presented. A set of eight steel frames are used for this purpose, four correspond to PTSF with semi-rigid connections and hysteretic dissipaters, which consist of 4, 6, 8 and 10 stories; the other four are SFWC with the same number of stories. Global response parameters, as maximum inter-story drift (γ), residual drift (γ_R), hysteretic energy (E_H), base shear force (V_b) and local response parameters as force and bending moment in beams and columns are compared. The responses were estimated using incremental nonlinear dynamic analysis. For this aim, the building frame models were subjected to a set of 30 narrow-band earthquake ground motions, which were scaled at different values of the seismic intensity in terms of spectral acceleration at first mode of vibration of the structure ($Sa(T_1)$). The selected seismic intensity values range from 0.1g to 2.0g with increments of 0.1g. In order to compare the performance, the average results obtained for each frame subject to the action of the 30 earthquakes is calculated. Results show that: the hysteretic energy dissipated in the PTSF is smaller than that dissipated in the corresponding SFWC. Under the action of severe earthquakes, plastic deformations in PTSF focus on the dissipater elements, preventing damage in beams and columns which remain in the elastic range. In all cases, inter-story drift and residual inter-story drift were smaller in the PTSF. Furthermore, in all PTSF γ_R was smaller than 0.005. The demand of strength in columns, such as axial force, bending moment, and shear is smaller in the PTSF too; this is more evident for the exterior columns. The shear and bending moment in beams are smaller in PTSF, but in the case of axial force higher values are observed in the PTST, this is caused by the additional post-tensioning force. In general, it can be concluded that PTSF are efficient to withstand seismic actions as they experience smaller distortion and resistance demands than their counterparts of frames with welded connections. The implication of this is that lighter sections could be used, reducing the total weight of the structure.

Keywords: hysteretic dissipaters; inter-story drift; residual drift; hysteretic energy; Post-Tensioned Steel Frames

1. Introduction

Post-tensioned steel frames (PTSF) with hysteretic dissipater, are an alternative to replace moment resistance steel frames with welded connections (SFWC) in seismic areas. Under the action of strong earthquakes plastic deformations are concentrated in the dissipaters elements, while the beams and columns remain in the elastic range. PTSF are structural systems proposed by Ricles [1] and have been studied for others researches [2, 3, 4, 5, 6, 7, 8, 9]. İn this kind of structure, connections are designed to prevent brittle fractures in the area of the nodes which can cause a strong reduction in ductility, as ocurred during the Northridge Earthquake in 1994.

The performance of the PTSF system is nonlinear due to the way it deforms, the beam-column joint remains "closed" under conditions of service and is "open" under the action of a strong earthquake. Dissipation of energy occurs in the items placed for that purpose, usually called energy dissipater systems (EDS). The dissipation mechanism might occurs by inelastic deformations or friction. Thereby damage is prevented in the beams and columns concentrating it on the EDS. The self-centering capability is supplied by the post-tensioned (PT) system, built with cables or rods of high strength steel, which are stretched in the elastic range. Since the connections are opened during severe earthquakes, tendons' length increases, in consequence, the elastic action tends to restore its original length, "closing" the connection after the earthquake. As a result, when a PTSF is properly designed, it can resist severe earthquakes, either without damage, or with little damage accumulated in the elements of the main structure, with reduced interstory drifts and without residual interstory drifts [10]. It is important to consider the residual interstory drifts in the seismic development of the structure. In SFWC large residual deformations are expected after a strong earthquake, which may cause undesired response during subsequent earthquakes, including the possibility of partial or total structural collapse. They also may increase the costs of repairing or replacement of non-structural elements, due to permanent deformation.

In order to quantify the difference between the seismic performance of FPSF and the SFWC, the frames are subjected to the action of 30 earthquakes; the mean of the maximum values are calculated for the following response parameters: hysteretic energy (E_H) in columns, beams and semi-rigid posttensioned connections; axial force, shearing force and bending moment in beams and columns; base shear; interstory drift and residual drift. Based on the results it can be estimated which kind of structure is more efficient to withstand strong earthquakes.

2. Structural models

Eight steel structural frames were analyzed in the study, four SFWC and four PTSF. The first group was designed according to the seismic requirements of RCDF [11], the buildings are assumed to be for office occupancy. They have 4, 6, 8 and 10-stories, 3 bays, hereafter identified as WCF4, WCF6, WCF8 and WCF10 respectively. The dimensions of the frames are shown in Fig. 2.1. The beams and columns are built of A36 steel W sections. A bilinear hysteretic model behavior with 3% of post-yielding stiffness was considered for the analyses and the damping used was 3% of critical. The fundamental periods of vibration (T_1) are 0.92, 1.09, 1.20 and 1.35 s respectively. The PTSF frames were designed according to the recommendations proposed by Garlock [7], which basically start with the design of the steel frames as usually is done (considering rigid connections), and then, the semi-rigid post-tensioned connections are designed to satisfy the requirements of the serviceability and resistance conditions. The beam-column connection consists of two angles bolted to the flanges of the beam and to the column flange (top and seat). The four PTSF models are identified here as PTF4, PTF6, PTF8 and PTF10, for the frames with 4, 6, 8 and 10 stories. They have fundamental periods of vibration of 0.89, 1.03, 1.23 and 1.37 s, respectively. It is noticed that the mechanical characteristics and dimensions of beams and columns are the same for both SFWC and PTSF. Fig. 2.2 shows a typical assembly of a post-tensioned steel frame, where the post-tensioned strands can be identified. The energy-dissipating elements (bolted angles) can also be observed.

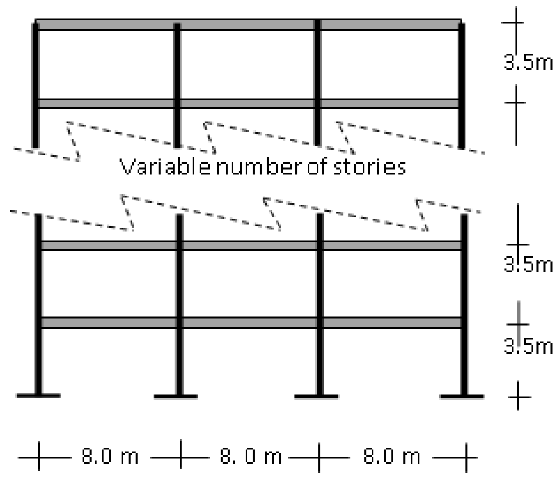

Figure 2.1. Overall dimensions the frames

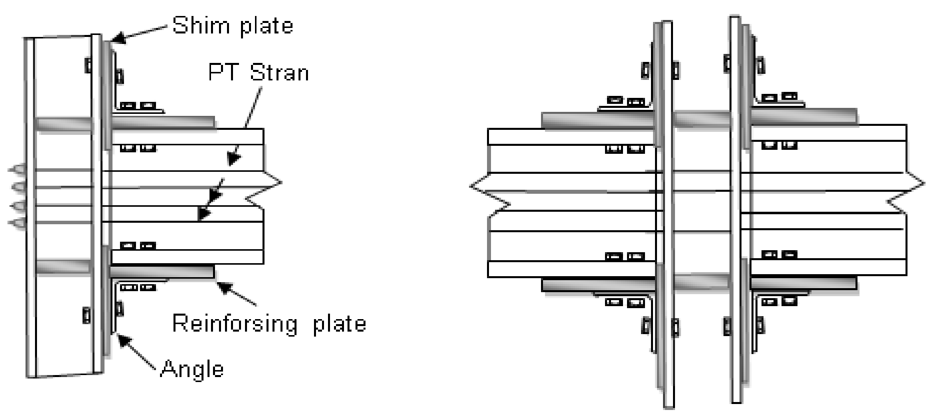

Figure 2.2. Angles and post-tensioned strands in PTSF

The hysteretic rules that represent the cyclic behavior of the connections of the PTSF are characterized by moment-rotation curves (M-θr), which usually present shapes similar to a flag. This representation characterizes the nonlinearity, self-centering capability and energy dissipation capacity of the connection. Experimental tests with isolated angles, subjected to cyclic and monotonic loads showed a stable cyclic response and good capability of hysteretic energy dissipation [12, 13]. Ultimate strength exceeds 3 times the yield strength and ductility reached values between 8 and 10. The strength and stiffness in bending of the post-tensioned connection is coming from the contribution of the angles of the connection and the post-tensioned strands. Wires and angles work as springs in parallel. In the system post-tensioned strands exhibit linear behavior, while connecting angles behave non-linear from the start of the deformation. Fig. 2.3 shows a typical example of a hysteretic curve corresponding to a post-tensioned connection, as well as decompression moments (*Md*) and the closing moment (*Mc*) of the connection. The mathematical expressions of the curves were obtained from the superposition of the exponential equation proposed by Richard [14] for semi-rigid connections and the linear contribution of the strands,. The curves obtained with the equations were compared with experimental results published by Ricles [2] and Garlock [6] exhibiting a good accuracy [13].

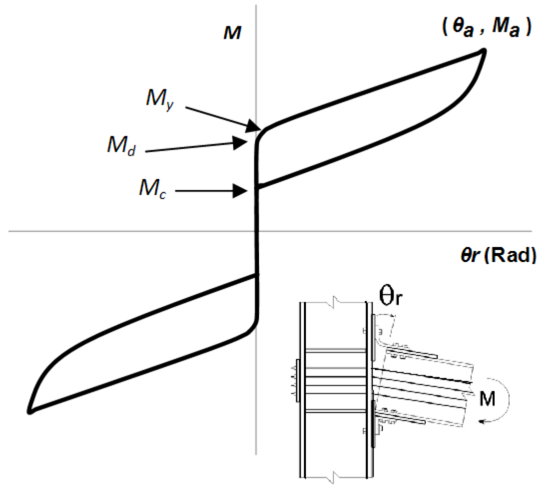

Figure 2.3. Moment-relative rotation curve of the connecting post-tensioned

3. Seismic ground motion

As stated earlier, the structural models described above were subjected to 30 long-duration narrow-band seismic records. The narrow-band ground motions have a special feature that significantly affects specific structures within a short interval periods (specially thus suffering of softening or those with structural periods close to the period of the soil). In fact, these records demand large amounts of energy to structures compared to movements of wide band [15]. The records were previously used by Bojórquez [16], and they correspond to the seismic subduction events. They were taken where the period of the soil was close to two seconds in sites where most of the damage during the México earthquake of September 19, 1985 occurred.

4. SFWC and PTSF comparison

The force, displacement and dissipated hysteretic energy of the traditional and post-tensioned steel frames were estimated using incremental nonlinear dynamic analysis [17]. For this aim, the building frame models were subjected to the set of 30 narrow-band earthquake ground motions, which were scaled at different values of the seismic intensity in terms of spectral acceleration at first mode of vibration of the structure $Sa(T_1)$. The selected seismic intensity values were from 0.1g to 2.0g with increments of 0.1g. The RUAUMOKO program [18] was used for the step by step nonlinear dynamic analysis. At the end of the earthquakes for each scaling levels, the results are expressed as the mean of the maximum value of inter-story drift (γ), residual drift (γ_R), base shear (Vb), axial force (P), shear force (V) and bending moment (M) of beams and columns, the E_H dissipated by columns ($E_H Col$), E_H dissipated by beams ($E_H Beam$) and E_H dissipated by connections ($E_H Conn$).

4.1 Hysteretic energy

The E_H mean calculated for each frame, subjected to the action of 30 earthquakes scaled for $Sa(T_1)$=1.0g is shown in Fig. 4.1. As be expected the magnitude of E_H increases if the number of stories increases, in all cases the E_H is lower for PTSF than for SFWC, this difference is more significant as the number of stories increases.

It is worth to highlight that the proper performance of the structures depends on how and where energy is dissipated. Figs. 4.2a-c show the E_H distribution of PTF10; in this case, columns, connections and beams dissipate 63%, 37% and 0% of the E_H total respectively. It can be observed in Fig. 4.2b, that E_H dissipated by columns at concentrated in the frame base and that there's no dissipation in the higher interstory, the reason for this is that columns are completely fixed and yield at the base even for moderate seismic intensities. In Fig. 4.2c it is shown that the connections dissipate energy in all the floors, the maximum values are located between 0.25 and 0.5 of the frame height and decrease for the upper floors. Fig. 4.3a-c shows the WCF10 results for the same seismic intensity discussed before, in this case the participation of columns decreases (19%) and beams are the ones that dissipate a higher value of E_H (81%); this is expected, because the frames were designed with the weak column-strong beam approach. As in the previous case only the columns of the base dissipate energy. The beams dissipate energy at all levels, peak demands occur at a height between 0.25 and 0.5 of the total height of the frame. Table 1 shows the ratio values of the total E_H of the PTSF to the total E_H for the SFWC of the frames of 4, 6, 8 and 10 levels (F4, F6, F8 y F10) for $Sa(T_1)$ of 0.5g, 1.0g, 1.5g y 2.0g, respectively.

The results show that in all cases the dissipated E_H for the PTSF is smaller than that of SFWC. The performance in all the frames for different $Sa(T_1)$ is similar to illustrated in Figs. 4.2 and 4.3. Thus, it can be concluded that PTSF have a better performance since most of the E_H is dissipated in the connection, with the advantage that if the dissipater elements are damaged can be easily replaced. On the other hand, even with the angles of the connection damaged due to fatigue, resilience and stiffness of the connection are not completely lost because the tendons still work in the elastic range.

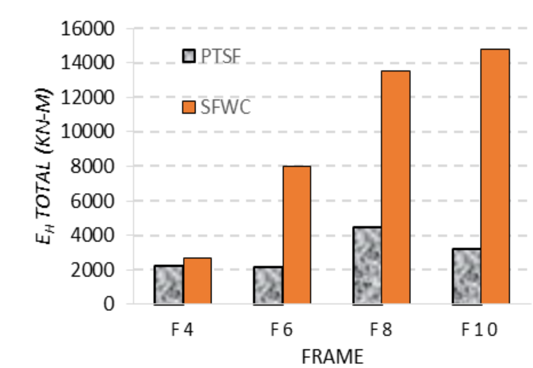

Fig. 4.1 E_H total para $Sa(T_1)$=1.0g

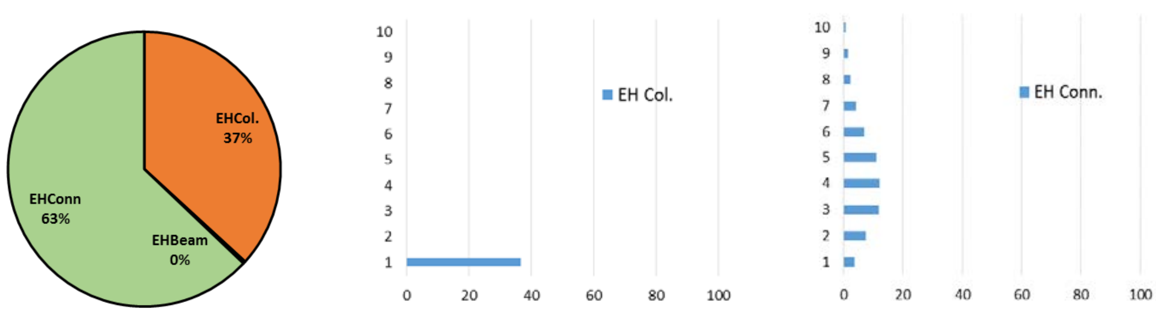

a) b) c)

Fig. 4.2 E_H en PTF10 with $Sa(T_1)$=1.5g. a) E_H total, b) E_H en columns, c) E_H en connections

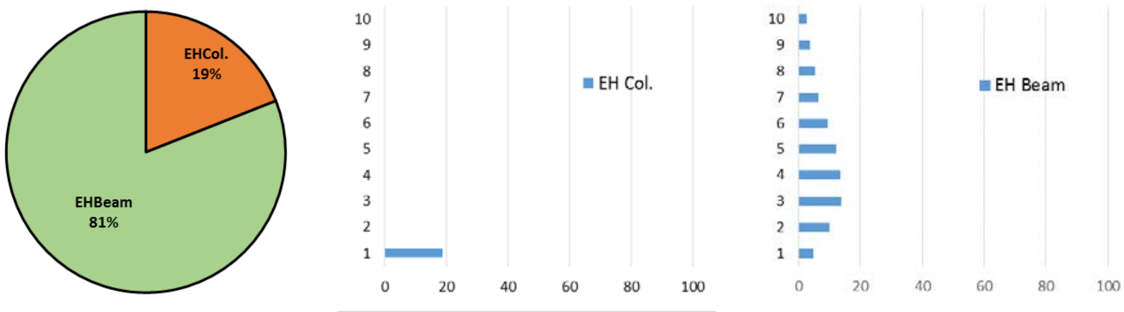

a) b) c)

Fig. 4.3 E_H en WCF10 with $Sa(T_1)$=1.5g, a) E_H total, b) E_H en columns, c) E_H en connections

Table 1 - E_H total de PTSF/SFWC

$Sa(T_1)$	0.5g	1.0g	1.5g	2.0g
F4	0.46	0.83		
F6	0.31	0.27		
F8	0.90	0.33	0.77	
F10	0.37	0.22	0.23	0.24

4.2 Drift and residual drift

The mean of γ is calculated for each frame and different values of $Sa(T_1)$. Fig. 4.4 shows the results for frames PTF10 and WCF10 for $Sa(T_1)$ of 0.5g, 1.0g, 1.5g y 2.0g. In all cases γ of PTF10 is smaller than that of WCF10. It is observed that γ follow a lognormal distribution though height, with maximum values on the 4th floor. The γ in WCF10 for $Sa(T_1)$ of 0.5g y 1.0g also has a lognormal distribution, but for higher values of $Sa(T_1)$ it is observed that the maximum distortions occur in the upper floors, this is due to increasing participation of higher modes on response of SFWC.

Table 2 shows the ratio $R\gamma$ of mean values of γ of the PTSF to the mean values of γ of the SFWC. In all cases it is observed that γ is smaller for the PTSF, with reductions of at least 60% as observed for the 10th floor. With the mean residual drifts calculated, is defined as ratio of the γ_R of the PTSF and the γ_R of the SFWC ($R\gamma_R$), Table 2 shows that in all cases γ_R values are smaller on the PTSF, decreasing 66% as observed in the first floor of F4. Also it is observed that in all the PTSF, γ_R is smaller than 0.5%, which is the limit to guarantee the comfort of the building users and to economically feasible repair the structure [19]. For these reasons, the results suggest that the PTSF are more efficient to control the seismic performance in terms of γ and γ_R. This applies to frames with different heights and different seismic intensities. It is worth to highlight that the reduction of γ implies smaller structural damage. Similarly, reducing γ_R implies a reduction of the repairmen cost and of the possibility of building interruption of operation of the building.

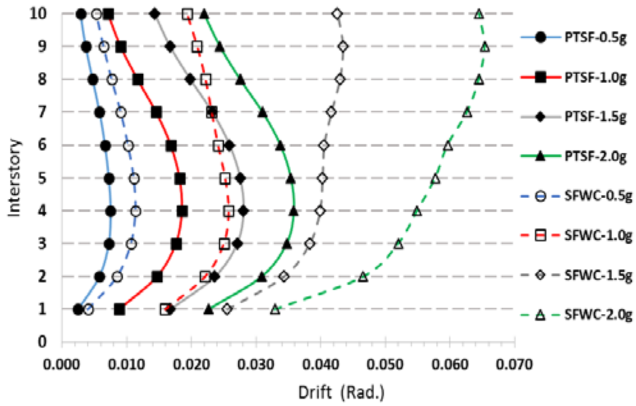

Fig. 4.4 Interstory drift F10

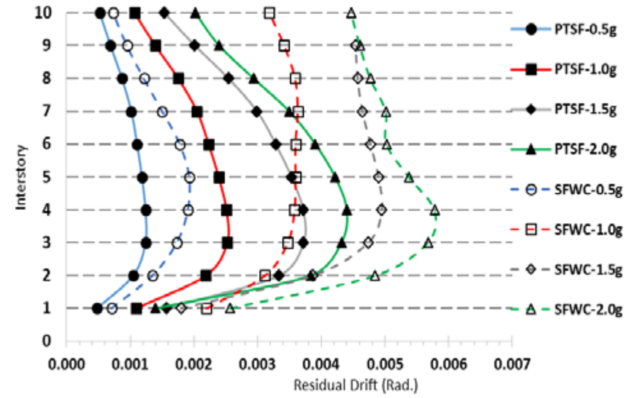

Fig 4.5 Residual interstory drift F10

Table 2 - $R\gamma$ y $R\gamma_R$ values

	story 1	story 2	story 3	story 4	story 5	story 6	story 7	story 8	story 9	story 10
	Interstory Drift									
$R\gamma F4$	0.81	0.81	0.76	0.69						
$R\gamma F6$	0.57	0.60	0.57	0.52	0.48	0.48				
$R\gamma F8$	0.79	0.83	0.82	0.77	0.70	0.64	0.59	0.55		
$R\gamma F10$	0.63	0.67	0.69	0.68	0.67	0.64	0.58	0.51	0.44	0.40
	Residual Interstory Drift									
$R\gamma_R F4$	0.34	0.49	0.51	0.53						
$R\gamma_R F6$	0.47	0.65	0.63	0.64	0.71	0.69				
$R\gamma_R F8$	0.70	0.89	0.82	0.77	0.74	0.71	0.69	0.64		
$R\gamma_R F10$	0.65	0.78	0.75	0.72	0.70	0.68	0.65	0.59	0.52	0.46

4.3 Forces and bending moments

In order to compare the performance of frames in terms of resistance, first the means of the maximum axial force (P) values, the bending moment (M), shear force (V) and the shear force resultant at the first interstory (V_b) are calculated for values of Sa(T_1) equals to 0.5g, 1.0g, 1.5g y 2.0g for all the frames. Then, the ration of the mean of the maximum values of these parameter for PTSF to those of SFWC is calculated. Results of given in Table 3 for some beams and columns. It is observed in most cases that V, M y V_b are smaller for PTSF beams, except for the model F4 for $Sa(T_1)$=1.0g. The axial force at interior columns is lightly higher for the PTSF and increase with increasing $Sa(T_1)$. It also occurs for most of the beams, noticing that for a giving value of $Sa(T_1)$ the increment is more significant for frames of lower height. The increment of the axial force in beams of PTSF is due to the compression action exerted by the post-tensioned elements. Finally, in all cases V_b is smaller in the PTSF, this reduction is more significant for the frames of greater height. In general, it can be concluded that the PTSF experience smaller resistance demands than their counterparts SFWC, implying that lighter sections may be used with consequent savings in weight.

Table 3 - Ratio values of the forces of the PTSF between the forces of the SFWC

FRAME	Columns						Girder						*Vb*
	Ext.			Int			Ext.			Int			
	P	*M*	*V*	*P*	*M*	*V*	*P*	*M*	*V*	*P*	*M*	*V*	
$Sa(T_1)$=0.5g													
F4	0.88	0.79	0.75	0.98	0.90	0.83	0.88	0.67	0.69	1.30	0.68	0.69	0.80
F6	0.78	0.65	0.63	1.08	0.78	0.78	0.47	0.66	0.64	0.70	0.66	0.65	0.73
F8	0.81	0.81	0.71	1.02	0.85	0.74	0.66	0.64	0.61	0.84	0.65	0.61	0.73
F10	0.81	0.70	0.65	1.01	0.75	0.71	0.48	0.65	0.63	0.65	0.65	0.63	0.67
$Sa(T_1)$=1.0g													
F4	1.08	1.19	1.11	1.03	1.22	1.15	2.51	0.96	0.99	4.33	0.97	0.98	0.94
F6	0.86	0.90	0.91	1.18	0.88	0.89	1.24	0.99	0.99	2.36	0.99	0.99	0.88
F8	0.87	0.96	0.86	1.09	0.90	0.81	1.25	0.77	0.74	2.38	0.77	0.74	0.82
F10	0.88	0.92	0.82	1.05	0.87	0.80	0.99	0.87	0.81	1.39	0.87	0.81	0.75
$Sa(T_1)$=1.5g													
F10	0.91	0.94	0.86	1.13	0.87	0.80	1.38	0.95	0.95	2.42	0.96	0.96	0.79
$Sa(T_1)$=2.0g													
F10	0.90	0.92	0.86	1.14	0.84	0.80	1.46	0.95	1.04	*2.86*	*0.96*	*1.03*	0.82

5. Conclusions

The seismic performance of eight steel frames, four post-tensioned with semi-rigid connections and dissipaters hysteretic (PTSF), and four with typical welded connections (SFWC) which are considered perfectly rigid is studied in this paper. The responses were estimated using incremental nonlinear dynamic analysis. A set of 30 narrow-band earthquake ground motions, which were scaled at different values of the seismic intensity in terms of $Sa(T_1)$ was considered. The relative performance of the PTSF and the SFWC can be summarized in three categories: 1) The PTSF are more efficient in terms of E_H dissipated. Most energy is dissipated by the angles at the connections avoiding damage in beams and columns that remain in the elastic range (except on the basis of the framework when the support is fixed). If angles in the connection is damaged after a strong earthquake, they can be replaced quickly and economically, returning to the structure to its original condition. On the other hand, despite the fact that the amount of E_H dissipated in the PTSF is much lower than that of its equivalent SFWC, has better performance in terms of the demands of distortions and resistance. This by the fact that is explained connections begin dissipating E_H since smaller seismic intensities, also they dissipate a more homogenous way throughout the frame avoiding concentrations that enable a mechanism of collapse. While it is important the magnitude of E_H structure can dissipate, for a good seismic performance, it is even more important how the energy is dissipated. 2) The interstory drift are lower in the PTSF, the reduction, with respect to the SFWC in the interstory with greater demand is 30%. The residual interstory drift are smaller in the PTSF with a 33% reduction in the interstory with greater demand; in all cases the γ_R is less than 0.005, which is considered as the limit to ensure the comfort of the occupants of the building and to have financially viable repairment. 3) The demands of resistance in terms of shear and bending moment are lower in PTSF, the axial force was slightly higher in some cases at the interior column of PTSF, and the axial force in beams was greater in most cases. This is explained by the additional axial force being transferred to the post-tensioned elements, which increases their strength when connections open as the frames move laterally. With the exception of the axial force in beams it can concluded that the strength demands are lower in FPSF. As a general conclusion it can be said that the seismic performance of the PTSF is better than their equivalents SFWC.

6. Acknowledgements

This study was supported by Secretaría de Educación Pública (PROMEP, DSA/103.5/15/7085), and by Universidad Autónoma de Sinaloa (PROFAPI 2014/109). Any opinions, findings, conclusions, or recommendations expressed in this publication are those of the authors and do not necessarily reflect the views of the sponsors.

7. Copyrights

8. References

[1] Ricles, J.M., Sause, R., Garlock, M.M. and Zhao, C. 2001. Post-tensioned seismic-resistant connections for steel frames, *ASCE Journal of Structural Engineering*, Vol. 127, No. 2, p. 113-121.

[2] Ricles, J.M., Sause, R., Peng, S.W. and Lu, L.W. 2002. Experimental evaluation of earthquake resistant post-tensioned steel connections, *ASCE Journal of Structural Engineering*, Vol. 128, No. 7, p. 850-859.

[3] Ricles, J.M., Sause, R., Lin, Y. C. and Seo, C. Y. (2010). "Self-Centering Moment Connections for Damage-Free Seismic Response of steel MRFs", *2010 structures congress ASCE*, 955-966

[4] Christopoulos, C., Filiatrault, A. and Uang, C.M. (2002a). "Self-centering post-tensioned energy dissipating (PTED) steel frames for seismic regions", University of California, Report No. SSRP-2002/06.

[5] Christopoulos, C., Filiatrault, A., and Uang, C.-M. (2003). "Seismic demands on post-tensioned energy dissipating moment-resisting steel frames." *Proc., Steel Structures in Seismic Areas (STESSA)*, Naples, Italy

[6] Garlock, M, Ricles, J., and Sause, R. (2005) "Experimental Studies on Full-Scale Post Tensioned Steel Connections", *Journal of Structural Engineering*, ASCE, **131**(3), 438-448.

[7] Garlock, M, Sause, R.and Ricles, J., (2007). "Behavior and Design of Posttensioned Stell Frames System" *Journal of Structural Engineering*, ASCE, **133**(3), 389-399.

[8] Rojas, P., Ricles, J.M. and Sause, R. (2005). "Seismic performance of posttensioned steel moment resisting frames with friction devices", *ASCE Journal of Structural Engineering*, Vol. 131, No. 4, p. 529-540.

[9] López-Barraza A., Ruiz S.E., Bojórquez E., Reyes-Salazar A., (2012). "Seismic performance of steel frames with pos-tensioned connections", *15 World Conference on Earthquake Engineering.*

[10] López-Barraza A, Edén Bojórquez, Sonia E. Ruiz and Reyes-Salazar A.(2013) "Reduction of Maximum and Residual Drifts on Posttensioned Steel Frames with Semirigid" Connections," *Advances in Materials Science and Engineering*, vol. 2013, Article ID 192484, 11 pages,. http://dx.doi.org/10.1155/2013/192484.

[11] RCDF 2004. Reglamento de Construcciones del Distrito Federal.

[12] Shen, J., and Astaneh-Asl, A. (1999). ''Hysteretic behavior of bolted angle connections.'' *J. Constr. Steel Res.*, **51**, 201–218.

[13] López-Barraza A (2014) Diseño sísmico de marcos de acero con conexiones semi-rígidas, basado en energía, *Ph.D. dissertation*, Universidad Nacional Autónoma de México, México City

[14] Richard, R.M. and Abbott, B.J. (1975). “Versatile elastic-plastic stress-strain formula”, *J. Eng. Mech. Div.*, **101**(4), 511-515.

[15] Terán-Gilmore, A. and Jirsa, J.O. (2007), “Energy demands for seismic design against low-cycle fatigue”, *Earthquake Engineering and Structural Dynamics*, **36**, 383-404

[16] Bojórquez, E., Ruiz S. E., & Terán-Gilmore A. 2008. Reliability-based evaluation of steel structures using energy concepts, *Engineering Structures* 30(6), pp. 1745-1759.

[17] Vamvatsikos D, Cornell CA (2002): Incremental dynamic analysis. *Earthquake Engineering & Structural Dynamics*, **31** (3), 491-514.

[18] Carr A. (2011) “RUAUMOKO” *Inelastic Dynamic Analysis Program*, University of Cantenbury, Department of Civil Engineering.

[19] McCormick, J., Aburano, H., Ikenaga, M. and Nakashima, M. (2008). “Permissible residual deformation levels for building structures considering both safety and human elements”, *14th Conference on Earthquake Engineering.* Beijing, China, 12-17 October.